ANALYSIS OF SIMULATED REFLECTION CHARACTERISTICS OF UNIFORM AND APODIZED FIBER BRAGG GRATINGS

E. Gemzický, J. Müllerová

Department of Engineering Fundamentals, Faculty of Electrical Engineering, University of Žilina, ul.kpt. J. Nálepku 1390, 031 01 Liptovský Mikuláš, Slovakia, mail: gemzicky@lm.uniza.sk

Summary In this paper, the simulations of the reflectance of the uniform and apodized fiber Bragg gratings (FBG) are presented. The simulations are based on the coupled–mode theory. The simulated reflectances of FBGs with different lengths and the modulations of the refractive index were described. The influence on the bandwidth of the reflected spectra at the Bragg wavelength and the maxima of the reflected energy were investigated. FBGs with several types of apodized variations of the refractive indices were modeled to show how the sidelobes can be supressed.

1. INTRODUCTION

The fiber Bragg grating (FBG) is an optical device with a periodic variation of the refractive index along the propagation direction in the core of the fiber. As the core of the optical fiber is due to the doping by germanium highly photosensitive, FBGs can be fabricated by the exposing the fiber core to UV radiation. This induces the changes of refractive index along the core of the fiber. The resulting refractive index changes depend on the UV light exposure and exposure pattern. Several techniques are commonly used to fabricate FBGs: the point-by-point technique, the interferometric technique and the phase mask technique [1-3].

FBGs take the advantages of a simple structure, low insertion loss, high wavelength selectivity, polarization insensitivity and full compatibility with general single mode communication optical fibers. Properly manufactured FBGs offer high reflectances (greater than 75% [4]) and narrow bandwidths at the Bragg wavelength. All this makes them suitable for applications in fiber optical communications, e.g. as WDM demultiplexers, fiber laser technique and fiber sensor system [2], e.g. for strain a temperature measurements.

This paper is devoted to the simulations of reflectance performances of the reflection FBGs with the average fiber core refractive index of 1.447. The refractive index modulation and the FBG length were changed to show the influence on the spectral reflectance of the Bragg wavelength of 1550 nm.

2. THE COUPLED-MODE THEORY

An FBG can be considered as a weakly coupled waveguide structure. The coupled-mode theory is most generally used to analyze the light propagation in a weakly coupled waveguide medium. The coupled-mode equations that describe the light propagation in the grating can be acquired by using the coupled-mode theory.

The refractive index modulation along the fiber axis z (Fig. 1) can be represented by the expression

$$n(z) = n_{av} V_n(z) \tag{1}$$

where n_{av} is the average refractive index of the fiber core, $V_n(z)$ is the modulation of the refractive index defined as

$$V_n(z) = g(z)\left[1 + v\cos\left(\frac{2\pi}{d}\cdot z\right)\right] \tag{2}$$

where $g(z)$ is the apodization function, d is the Bragg grating period and v is the fringe visibility. According to Eq. 2, the modulation of the refractive index V_n depends on the apodization function $g(z)$.

A small amount of the incident light energy is reflected at each periodic refractive index change (Fig. 1). Then we have either the reflection FBG of the transmission FBG. The reflection FBGs work properly with shorter Bragg grating periods whilst the transmission FBGs are long-period gratings.

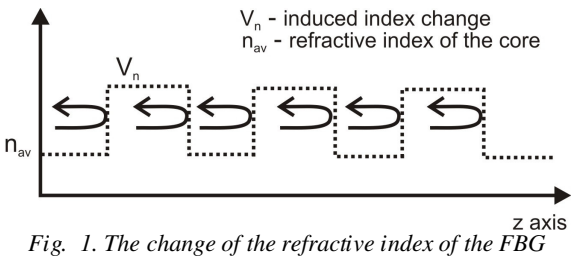

Fig. 1. The change of the refractive index of the FBG

All reflected light waves are combined into the one reflected at a particular wavelength that is related to the Bragg condition defined by

$$\lambda_{Bragg} = 2 \cdot n_{av} \cdot d \tag{3}$$

The wavelength λ_{Bragg} at which this reflection occurs is called the Bragg wavelength and depends on the refractive index and the Bragg grating period d. Longer periods can be used to achieve the broader bandwidth and FBGs of this type are called long-period FBGs. They typically have Bragg grating periods of the order from ~100 micrometers to a millimeter.

Only the wavelengths that satisfy Eq. 3 are reflected. The reflectance of the input light achieves a peak at the Bragg wavelength.

The characteristics of the FBG reflected spectrum can be modelled by several methods. The basic idea of the coupled-mode theory is that electrical field of the optical fiber with the variation of the refractive index can be represented by the linear combination of the modes of the field distribution without variations [5, 6].

The modal fields of the optical fiber can be represented by

$$E_{\pm j}(x, y, z) = e_{\pm jt}(x, y) \cdot \exp(\pm i\beta_j z) \quad j = 1,2,... \quad (4)$$

where $e_{\pm jt}$ is the amplitude of transverse electric field of the j^{th} propagation mode and ± symbolizes the direction of the propagation. β_j is called the propagation constant. Next we assume a time dependence *exp(-iωt)*. The transverse component of the electric field at position *z* in the variable fiber can be described by the linear superposition of the ideal guided modes of the invariable fiber. That can be written as

$$\vec{E}_t(x, y, z, t) = \sum_j \begin{bmatrix} A_j^+(z) \cdot \exp(i\beta_j z) \\ + A_j^-(z) \cdot \exp(-i\beta_j z) \end{bmatrix} \cdot \vec{e}_{jt}(x, y) \cdot \exp(-i\omega t) \quad (5)$$

Where $A_j^+(z)$ and $A_j^-(z)$ are slowly varying amplitudes of the j^{th} backward and forward travelling waves respectively and $\vec{e}_{jt}(x, y)$ is the transverse mode field. The coupled-mode equations can be simplified in the two modes that they are described as [6]

$$\frac{dR(z)}{dz} = i\hat{\sigma}(z)R(z) + ik(z)S(z) \quad (6)$$

$$\frac{dS(z)}{dz} = -i\hat{\sigma}(z)R(z) - ik^*(z)R(z) \quad (7)$$

$R(z) = A^+(z)\exp[i(\delta z - \phi/2)]$ is the forward mode and $S(z) = A^-(z)\exp[-i(\delta z + \phi/2)]$ is the reverse mode. $\hat{\sigma}$ is a general "DC" self-coupling coefficient called the local detuning and $k(z) = \frac{\pi}{\lambda} V_n(z) g(z) v$ is the "AC" coupling coefficient – local grating strength. The coupled-mode Eq. 6, 7 are used in the simulation of the spectral response of the FBG. Local grating strength and local detuning are fundamental parameters in the calculation of the spectral response of the FBGs. The general "DC" self-coupling coefficient $\hat{\sigma}$ can by described by

$$\hat{\sigma} = \delta + \sigma - \frac{1}{2}\frac{d\phi}{dz} \quad (8)$$

where $\frac{1}{2}\frac{d\phi}{dz}$ describes possible chirp of grating period and ϕ is the grating phase. The detuning δ can by described by

$$\delta = 2\pi n_{av}\left(\frac{1}{\lambda} - \frac{1}{\lambda_{Bragg}}\right) \quad (9)$$

For uniform FBGs, the chirp $\frac{d\phi}{dz}$ equal zero and the local detuning equals the detuning δ. The reflected amplitude spectrum can be obtained and described by

$$r(\lambda) = \frac{k^2 \sinh^2(\gamma_B L)}{\hat{\sigma}^2 \sinh^2(\gamma_B L) + \gamma_B^2 \cosh^2(\gamma_B L)} \quad (10)$$

where $r(\lambda)$ is the amplitude reflectance and $\gamma_B = \sqrt{k^2 - \hat{\sigma}^2}$ if $k^2 > \hat{\sigma}^2$ or $\gamma_B = i\sqrt{\hat{\sigma}^2 - k^2}$ if $k^2 < \hat{\sigma}^2$.

3. THE AMPLITUDE REFLECTANCE OF FIBER BRAGG GRATINGS

The reflectance spectra of the reflection FBGs were MATLAB simulated according to the Eq. 10. The effective refractive index n_{av} and the Bragg grating period *d* are constant for the uniform Bragg grating (*g(z)* = const) and the Bragg wavelength λ_{Bragg} = 1550 nm. The bandwidth $\Delta\lambda_{Bragg}$ at the Bragg wavelength at -50 dB and the amplitude reflectance r_{Bragg} at the Bragg wavelength were investigated. Fig. 2 shows the amplitude reflectance of a uniform FBG for three different lengths of the FBG with the following parameters: *d*=535.59 nm, n_{av}=1.447, V_n=3.10^{-4}. The bandwidth $\Delta\lambda_{Bragg}$ =0.5 nm for *L*=5 mm, $\Delta\lambda_{Bragg}$ =0.32 nm for *L*=10 mm and $\Delta\lambda_{Bragg}$ =0.24 nm for *L*=20 mm. The simulations show that the increase of *L* results in the reduction of the bandwidth by 1550 nm and in the increase of r_{Bragg}. The sidelobes are present on both sides of the peak at the Bragg wavelength that are undesirable for communication and sensor applications.

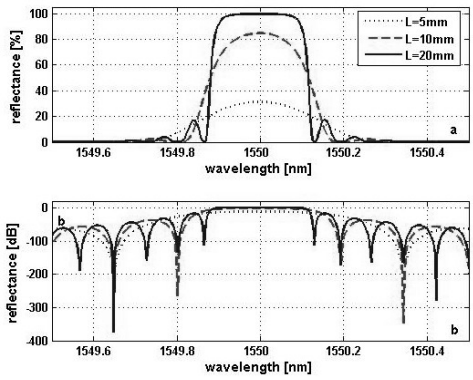

Fig. 2. Calculated reflectances (a [%], b [dB]) of the uniform FBG (g(z)=const). and variable L, d=535.59 nm, n_{av}=1.447, V_n=3.10^{-4}

Then we investigated the influence of the refractive index modulation V_n on the amplitude reflectance spectra of the FBG with the uniform Bragg grating for three different parameter V_n of the FBG with the following parameters: *d*=535.59 nm, n_{av}=1.447, *L*=10 mm (Fig. 3).

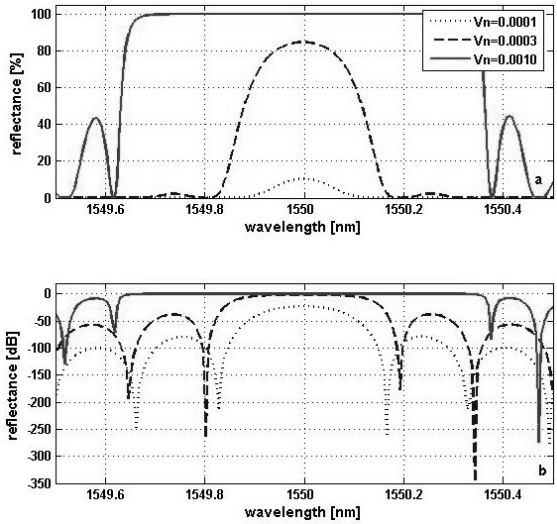

Fig. 3. Calculated reflectances (a [%], b [dB]) of the uniform FBG (g(z)=const.) for variable V_n, d=535.59 nm, n_{av}=1.447, L=10 mm

Three different values of the modulation of the refractive index V_n were used in the simulations. The simulation shows that the modulation V_n affects not only the bandwidth, but the maximum reflectance in λ_{Bragg} too. The increase in V_n causes the increase in r_{Bragg}, which is highly desirable for reflection FBGs. On the other hand, at the same time the bandwidth $\Delta\lambda_{Bragg}$ rises which could be harmful for WDM demultiplexers. We notice that at V_n=3.10^{-4}, the reflectance r_{Bragg}=83% and the bandwidth $\Delta\lambda_{Bragg}$=0.34 nm, whereas at V_n=1.10^{-3} r_{Bragg}=100%, $\Delta\lambda_{Bragg}$=0.74 nm. Therefore, in this case the optimization is recommended for a specific application.

FBGs with the uniform index profile as the WDM demultiplexers are reported to suffer from high crosstalk level [7, 8] especially due to the sidelobe existence. Two types of refractive index profile – the Gaussian profile and the sinc profile - were inserted into the simulation to show that the level of the undesirable sidelobes can be decreased. The apodized refractive index represents the situation when the function vanishes smoothly at the edges of the grating. Then the sidelobes decay and the crosstalk between two adjacent channels can be reduced.

The Gaussian-apodized profile is described by

$$g(z) = \exp\left[-a\cdot\left(\frac{z-L/2}{L}\right)^2\right] \qquad (11)$$

where *a* is the Gauss width parameter. The simulated reflectance spectrum is in Fig. 4. We notice that the reflectance r_{Bragg} = 100% and $\Delta\lambda_{Bragg}$=0.44 nm.

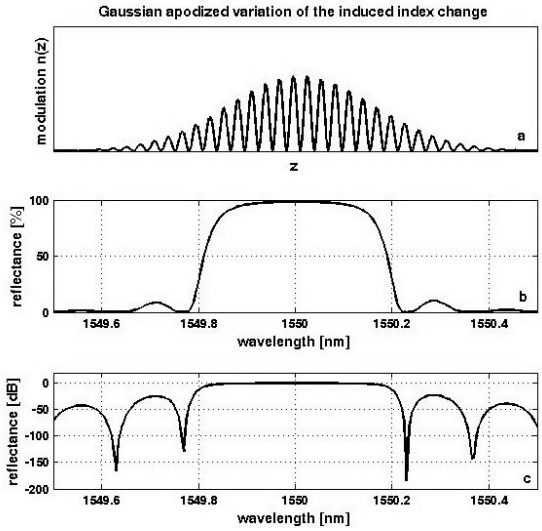

Fig. 4. The Gaussian- apodized index profile (a), the calculated reflectance [%] (b), [dB] (c)

The apodized refractive index profile described by the sinc function is characterized by more significant compression of the refractive index at the edges of the FBG than the Gaussian profile (Fig. 4, 5). The sinc-apodized profile is defined by the function

$$g(z) = \mathrm{sinc}(\pi\cdot(z-L/2)) \qquad (12)$$

For this index profile (Fig. 5) a considerable reduction of sidelobes was achieved and the bandwidth $\Delta\lambda_{Bragg}$ = 0.26 nm. Therefore, FBGs of

this type are suitable candidates for WDM demultiplexers with low crosstalk.

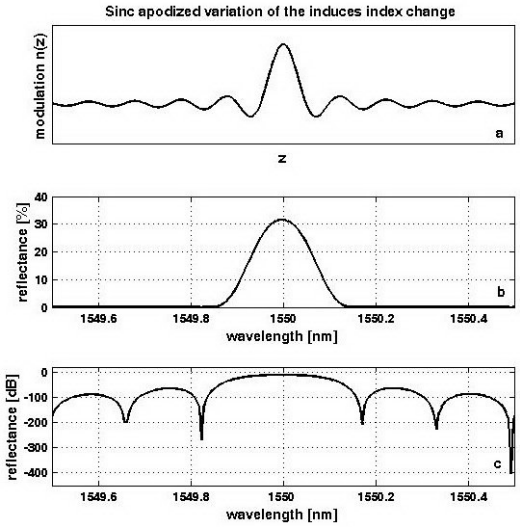

Fig. 5. The sinc-apodized index profile (a), the calculated reflectance [%](b), [dB] (c)

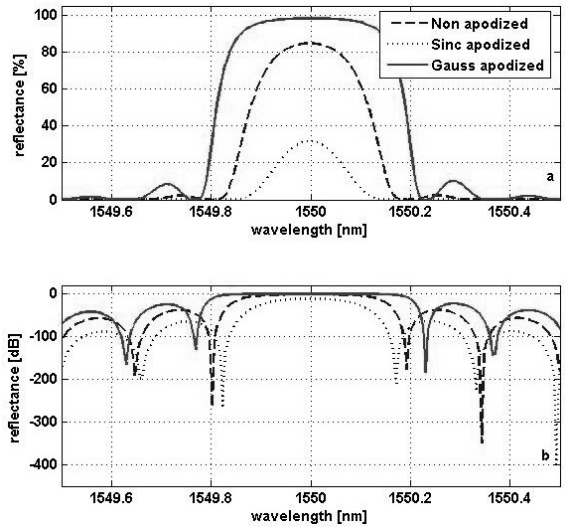

Fig. 6. The comparison of the calculated reflectance (a [%], b [dB]) of the FBG of the uniform index profile, the Gaussian and the sinc apodization.

The comparison of the amplitude reflectance of uniform (non-apodized), Gaussian-apodized and sinc-apodized FBGs is shown in Fig.6. Note that the most narrow reflected spectral band with suppressed sidelobes is achieved by the sinc-apodized FBG, although the reflectance in λ_{Bragg} is reduced in comparison with for FBGs of uniform or Gaussian profile.

4. CONCLUSION

In this paper reflectances of FBGs with different grating lengths and different modulations of the refractive index were simulated. The results show that the increase of the grating length causes the bandwidth decrease and the increase of the reflectance at the Bragg wavelength. When the refractive index modulation increases, then the reflectance and the bandwidth increase too. Although the reflectance at the Bragg wavelength of the sinc-apodized grating is reduced in comparison with the non-apodized FBG, a considerable reduction of the sidelobes and of the bandwidth at the Bragg can be achieved. This could be of interest for narrow-band wavelength selective filtering.

Acknowledgement
This work was partly supported by the Slovak Research and Development Agency under the project APVV COST-0041-06.

REFERENCES

[1] ERDOGAN, T.: *Fiber grating spectra.* Journal of Lightwave Technology, vol.15, no.8, 1997, pp. 1277-1294

[2] OUELLETTE, F.: *Fiber Bragg gratings*. Spie's Oemagazine – The SPIE Magazine of Photonics Technologies and Applications, vol.1, no.1, 2001, pp. 38-41

[3] ROSTAMI, A., YAZDANPANAH-GOHARRIZI, A.: *A new method for classification and identification of comples fiber Bragg garting using genetic algorithm.* Progress in Electromagnetic Research, PIER 75, 2007, 329 - 356

[4] KANG, Y., YE, CH., LUO, Z., SI, M.: *Investigation on reflection spectra of chirped and phase-shifted fiber Bragg gratings.* Optoelectronics letters, vol.3, no.2, 2007, pp. 112-114

[5] RABIN, M., W., SWANN, W., C., GILBERT, S., L.: *Interleaved, sampled fiber Bragg gratings for use in hybrid wavelength references*. Applied optics, vol.41, no.34, 2002, pp. 7193-7196

[6] MOKHTAR, M. R.: *Bragg grating filters for optical networks.* Thesis submitted for the degree of Doctor of Philosophy, University of Southampton, Faculty of Engineering, Science and Mathematics, January 2005

[7] DO, D.-D., LEE, K.-Y., KIM, N.: *Low-crosstalk demultiplexer based on apodized volume holographic grating.* International Workshop on Photonic Applications Hanoi, Vietman, 2004, pp. 175-179

[8] PHING, H. S., ALI, J., RAHMAN, R. A., TAHIR, B., A.: *Fiber Bragg grating modeling, simulation and characteristics with different gating length.* Journal of Fundamental Sciences 3 (2007) pp. 167 - 175